AFRL-VA-WP-TR-1998-3092

DEVELOPMENT OF FILTERED RAYLEIGH SCATTERING VELOCIMETRY FOR WIND TUNNEL APPLICATION

C. D. CARTER

INNOVATIVE SCIENTIFIC SOLUTIONS, INC.
2786 INDIAN RIPPLE ROAD
DAYTON, OH 45440-3638

FEBRUARY 1998

FINAL REPORT FOR 04/14/1997 – 01/13/1998

THIS IS A SMALL BUSINESS INNOVATION RESEARCH (SBIR) PHASE I REPORT

AIR VEHICLES DIRECTORATE
AIR FORCE RESEARCH LABORATORY
AIR FORCE MATERIEL COMMAND
WRIGHT-PATTERSON AIR FORCE BASE OH 45433-7542

NOTICE

USING GOVERNMENT DRAWINGS, SPECIFICATIONS, OR OTHER DATA INCLUDED IN THIS DOCUMENT FOR ANY PURPOSE OTHER THAN GOVERNMENT PROCUREMENT DOES NOT IN ANY WAY OBLIGATE THE US GOVERNMENT. THE FACT THAT THE GOVERNMENT FORMULATED OR SUPPLIED THE DRAWINGS, SPECIFICATIONS, OR OTHER DATA DOES NOT LICENSE THE HOLDER OR ANY OTHER PERSON OR CORPORATION; OR CONVEY ANY RIGHTS OR PERMISSION TO MANUFACTURE, USE, OR SELL ANY PATENTED INVENTION THAT MAY RELATE TO THEM.

THIS REPORT IS RELEASABLE TO THE NATIONAL TECHNICAL INFORMATION SERVICE (NTIS). AT NTIS, IT WILL BE AVAILABLE TO THE GENERAL PUBLIC, INCLUDING FOREIGN NATIONS.

THIS TECHNICAL REPORT HAS BEEN REVIEWED AND IS APPROVED FOR PUBLICATION.

CONTRACT MONITOR, THOMAS J. BEUTNER
AFRL/VAAC

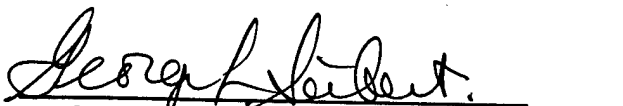

GEORGE SEIBERT, BRANCH CHIEF
AFRL/VAAC

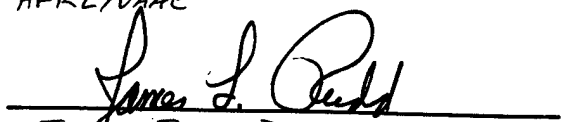

JAMES RUDD, DIVISION CHIEF
AFRL/VAA

Do not return copies of this report unless contractual obligations or notice on a specific document requires its return.

REPORT DOCUMENTATION PAGE

Form Approved
OMB No. 0704-0188

1. AGENCY USE ONLY *(Leave blank)*	2. REPORT DATE	3. REPORT TYPE AND DATES COVERED
	FEBRUARY 1998	FINAL REPORT 04/14/1997 -- 01/13/1998

4. TITLE AND SUBTITLE
DEVELOPMENT OF FILTERED RAYLEIGH SCATTERING VELOCIMETRY FOR WIND TUNNEL APPLICATION

5. FUNDING NUMBERS
C F33615-97-C-3004
PE 65502
PR 3005
TA FI
WU OJ

6. AUTHOR(S)
C. D. CARTER

7. PERFORMING ORGANIZATION NAME(S) AND ADDRESS(ES)
INNOVATIVE SCIENTIFIC SOLUTIONS, INC.
2786 INDIAN RIPPLE ROAD
DAYTON, OH 45440-3638

8. PERFORMING ORGANIZATION REPORT NUMBER
3004 FINAL

9. SPONSORING/MONITORING AGENCY NAME(S) AND ADDRESS(ES)
PROPULSION DIRECTORATE
AIR FORCE RESEARCH LABORATORY
AIR FORCE MATERIEL COMMAND
WRIGHT-PATTERSON AFB, OH 45433-7251
POC: DR. THOMAS J. BEUTNER, AFRL/VAAO, 937-255-2809

10. SPONSORING/MONITORING AGENCY REPORT NUMBER
AFRL-VA-WP-TR-1998-3092

11. SUPPLEMENTARY NOTES
THIS IS A SMALL BUSINESS RESEARCH INNOVATION (SBIR) PHASE I REPORT

12a. DISTRIBUTION AVAILABILITY STATEMENT
APPROVED FOR PUBLIC RELEASE, DISTRIBUTION UNLIMITED

12b. DISTRIBUTION CODE

13. ABSTRACT *(Maximum 200 words)*

THIS REPORT DEVELOPED UNDER SBIR CONTRACT
The goal of this SBIR program was to develop a FRS (filtered Rayleigh scattering) velocimetry instrument for the study of unsteady flowfields. During Phase I we constructed a single-velocity-component device for use with a single-mode Q-switched Nd:YAG laser. This FRS device included a custom wavemeter for recording accurately the laser wavelength on each pulse, two 16-bit, back-illuminated CCD cameras, and custom Windows-95 software for integrating the wavemeter and cameras. Initially, we tested and debugged the FRS system using a supersonic (Mach 1 . 36) axisymmetric jet. These tests demonstrated that accurate mean (within 5%) and instantaneous (within 4%) velocities can be obtained with this technique. Subsequent to these tests, we implemented the FRS velocimetry instrument in the SARL (Subsonic Aerodynamic Research Laboratory) wind tunnel to test the feasibility of applying this advanced instrumentation in a realistic large-scale tunnel facility. We investigated the flow over a delta-wing model with and without tail fins; here, the freestream velocity compared well to the value derived from pitot probes, while FRS measurements over the delta wing provided new insight into complex, unsteady flows. Potential applications include the timely and cost-efficient testing of novel aerodynamic concepts and designs in large-scale wind tunnels.

14. SUBJECT TERMS
SBIR REPORT
FRS, PDV, DGV, Filtered Rayleigh Scattering , Velocimetry, Planar Doppler Velocimetry, Doppler Global Velocimetry, Laser Diagnostics

15. NUMBER OF PAGES
21

16. PRICE CODE

17. SECURITY CLASSIFICATION OF REPORT	18. SECURITY CLASSIFICATION OF THIS PAGE	19. SECURITY CLASSIFICATION OF ABSTRACT	20. LIMITATION OF ABSTRACT
UNCLASSIFIED	UNCLASSIFIED	UNCLASSIFIED	SAR

TABLE OF CONTENTS

LIST OF ILLUSTRATIONS

1. INTRODUCTION

This final report describes R&D efforts on Air Force Contract F33615-97-C-3004 during the period 14 April 1997 to 13 January 1998. Contributing to the program effort were Drs. Campbell Carter and William Weaver of Innovative Scientific Solutions, Inc., and Prof. Gregory Elliott of Rutgers University (consultant).

Background

Popular two-dimensional velocimetry techniques include planar laser-induced fluorescence (PLIF) and particle imaging velocimetry (PIV). To apply PLIF, one must seed the air with a gas having appropriate electronic transitions, since neither N_2 nor O_2 is a reasonable probe species for large facilities. In small-scale facilities, I_2 and NO have been employed because of their amenable spectroscopy and good fluorescence yields. Employing these gases in larger facilities is impractical, however, because of their toxic and corrosive properties. In any event, the use of any seed gas in a large-scale facility would be prohibitively expensive because of the quantity that would be required. As a result of its inherent simplicity, PIV is being widely applied in many research facilities, in both subsonic and supersonic regimes. For large-scale wind-tunnel applications, however, PIV has the following disadvantages: 1) the accuracy can be poor when the out-of-sheet particle displacement is large; 2) if the span of the interrogation region is large ($\geq$ 0.5 m), the sheet irradiance is reduced as is the ability to image single particles; and, 3) application of correlation techniques is best suited to moderate and uniform seed levels (i.e., these techniques cannot be applied where the seed density is too high or too low, and seed-density boundaries can degrade accuracy). A new class of molecular-filter-based diagnostics, which we call filtered Rayleigh scattering (FRS), may overcome the limitations associated with PLIF and PIV for large-scale facilities. This SBIR research and instrument-development program will directly influence this capability.

Shimizu et al. [1983] first applied a molecular filter to eliminate large particle scattering in LIDAR thermometry; later Miles et al. [1991] and Meyers and Komine [1991] demonstrated the efficacy of employing laser scattering and an I_2 filter for flow diagnostics. The molecular/atomic filter, which is placed in front of the recording device (e.g., a charge-coupled device, CCD, camera), is simply a cylindrical optical cell (made from Pyrex, for example) containing a molecular

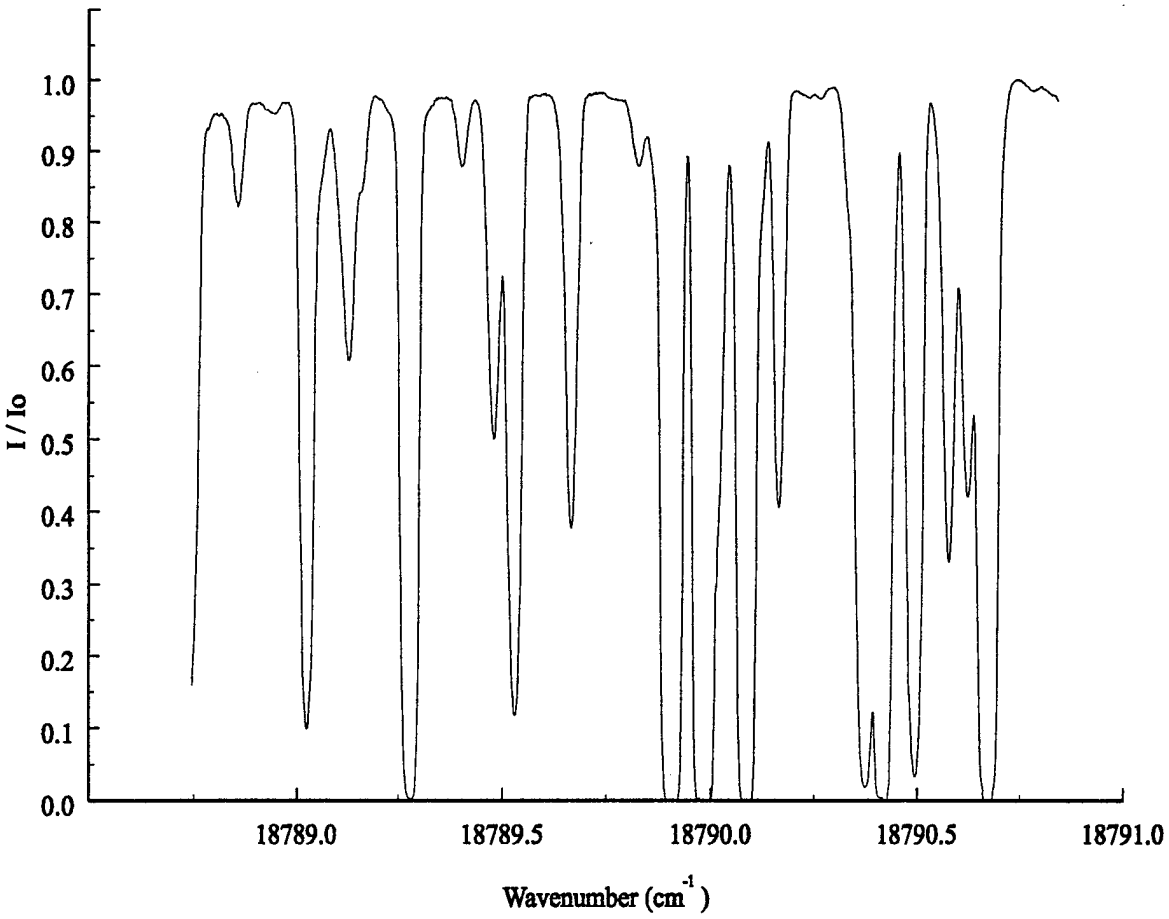

Figure 1. Iodine absorption lines in the tuning range of a Nd:YAG laser.

or atomic gas having absorption lines within the frequency tuning range of the interrogation laser. With the second harmonic of a Q-switched injection-seeded Nd:YAG laser (λ = 532 nm), the pulse duration is ~6 ns, while the linewidth is narrow and approximately transform-limited (~100 MHz); furthermore, the frequency can be tuned to any one of several absorption lines of I_2 (Fig. 1). This short pulse effectively freezes the fluid motion and allows recording of effectively instantaneous snapshots of the flowfield. To record velocity, one must measure the Doppler frequency shift (Hz):

$$\Delta f_D = \frac{1}{\lambda}(\mathbf{k}_s - \mathbf{k}_0)\cdot \mathbf{V}$$

Here $\mathbf{k}_s$ and $\mathbf{k}_0$ are the respective observed and incident unit wave vectors, $\mathbf{V}$ is the flow velocity vector, and λ is the wavelength of the incident light. In our application of FRS velocimetry, separate filter and reference cameras are used. The filter camera has a pressure-broadened I_2 filter

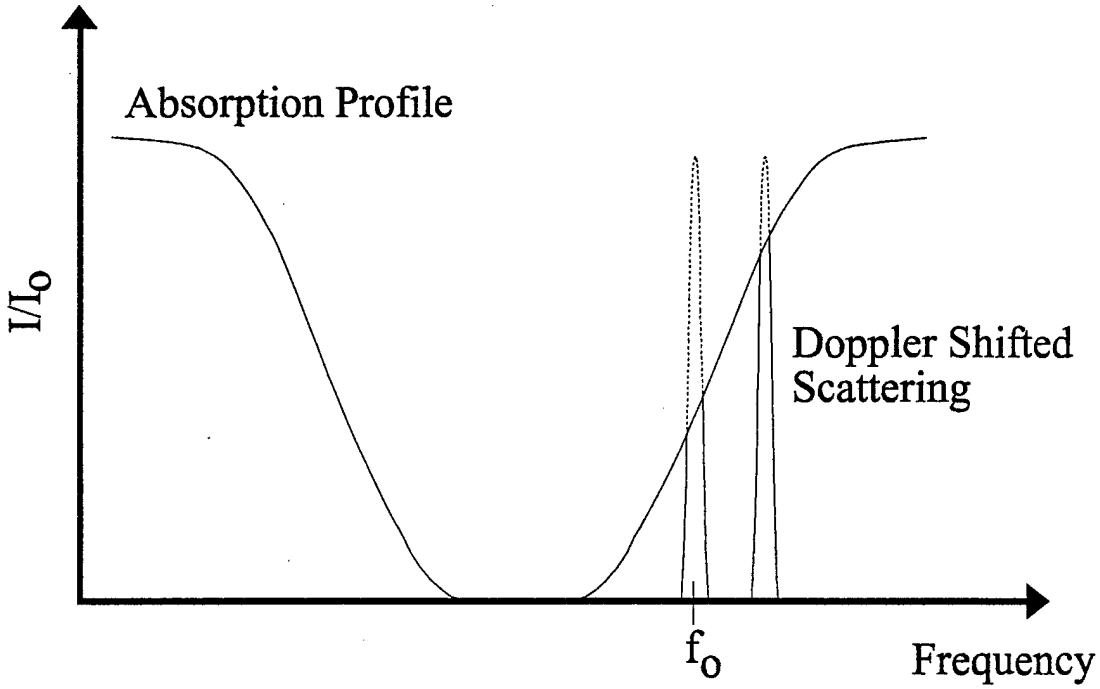

Figure 2. Schematic illustrating Filtered Rayleigh Scattering Velocimetry.

placed in front of it. Pressure broadening, the result of adding N_2, for example, to the cell, reduces the sensitivity of the filter transmission to changes in frequency (and, thus, Doppler shift); consequently, one can tailor the filter absorption-vs.-frequency characteristics to the requirements of a particular experiment. The reference camera records an image that is not affected by the filter; this image is then used to normalize that from the filter camera, accounting for variations in laser intensity and the particle size and density in the flowfield. When the laser frequency is tuned in the sloping region, the Doppler shift will move the scattered intensity in the absorption profile, resulting in an increase or decrease in the transmission (Fig. 2). Thus, when the transmission ratio is calculated from the filter and reference images, the velocity can be obtained. Although this technique has most often been applied to high-speed flows, McKenzie [1996] has estimated that a lower limit of detection of ~2 m/s (with current technology) is feasible.

The purpose of this Phase I SBIR program was to address instrumentation problems associated with the rapid evaluation and testing of wind-tunnel models. In particular, the capability of making fast, detailed, and accurate measurements of the off-body velocity field surrounding a wind-tunnel model is crucial to timely evaluation of innovative aerodynamic devices

for flow control, drag reduction, and lift augmentation. Many advanced aerodynamic designs result in complex, unsteady flowfields that are currently difficult or impossible to model. Even in cases where computational modeling is feasible, validation is a critical step in the design process. In both cases, reliable and efficient evaluation of these new aerodynamic designs will depend on the development of likewise reliable and efficient—and, therefore, cost-effective—wind-tunnel instrumentation. Because of the limitations of classical instrumentation (e.g., intrusiveness, time response, etc.) and advances in lasers and digital cameras, a FRS velocimetry instrument was developed and demonstrated. The specific accomplishments for this Phase I program included as follows:

1. We designed and implemented a single-velocity-component FRS instrument capable of resolving velocities within a few meters per second. This instrument included:

   a. Two back-illuminated 16-bit scientific-grade CCD cameras (one for recording the filtered scattering image and the second for recording the reference image). These thermoelectrically cooled detectors were configured to digitize the signals at 100 or 450 kHz rates; the RMS readout noise is less than 20 electrons at 450 kHz and less than 9 electrons at 100 kHz. Furthermore, the cameras included fiber-optic coupling to the PC.

   b. A custom laser wavemeter composed of two Stanford Research Systems gated integrators and photodiodes and a reference I_2 cell for recording, on a shot-by-shot basis, the laser wavelength. The integrated photodiode signals were digitized with 12-bit resolution by a Stanford Research Systems computer interface. This computer interface (which communicated to the PC via an IEEE 488 port) was also employed to open and close the mechanical shutters on the CCD cameras.

   c. I_2 cells with temperature controllers. The I_2 cells were designed such that the I_2 reservoir could be sealed from the main body, thus fixing the I_2 number density within the main body (and making the I_2 number density insensitive to ambient conditions). However, at the time of the wind tunnel tests, only one of this type of cell was available. Employing this type of cell design is critical to the development of a robust instrument.

2. We wrote menu-driven Windows 95 software to integrate the CCD cameras with the custom laser wavemeter. The software, written in the C programming language and with the aid of

National Instruments LabWindows/CVI package, allows the user to record instantaneous filtered and reference images synchronously with the laser wavelength inferred from the custom wavemeter.

3. We tested and "de-bugged" the single-component planar velocimetry system in a small-scale (1-cm-diameter) supersonic axisymmetry jet. With this facility, we were able to evaluate sources of error and single-shot noise.

4. In the SARL (subsonic aerodynamic research laboratory), we recorded a single velocity component above a sharp-leading-edge delta wing with and without tails. The inlet Mach number was set to 0.2.

2. WORK ACCOMPLISHED

In general, tests with FRS velocimetry have focused on feasibility studies and/or laboratory-scale experiments with the measurement of one or two components. Further work is needed to transition this promising technology from a laboratory technique with potential for accurate velocity measurements to a reliable engineering tool.

Selection and Configuration of Hardware

CCD Detectors

The initial part of this program involved the specification and purchase of two 16-bit, scientific-grade CCD cameras (512-by-512-pixel array) from PixelVision (Beaverton, OR). The system chosen includes a thermoelectrically cooled, back-illuminated CCD detector. Back-thinned/back-illuminated CCDs have high quantum efficiencies, nearly 90% at 532 nm. Furthermore, effective cooling and correlated sampling lead to low readout noise; at 100 kpixel/s readout rate, the RMS noise specification was 8-9 electrons with both cameras. The cameras were specified to have user-selectable readout rates of 100 and 450 kpixel/s; the higher readout rate is effective in reducing the data-acquisition times, and the lower value results in lower readout noise (the readout noise scales with the square root of the readout rate). The cameras were designed to have analog-to-digital gains of about 4.5 electrons per count. Thus, with 16-bit digitization—the full-well potential of the CCD is about 3×10^6 electrons—the camera's light-measurement dynamic range is greater than 10,000.

To simplify implementation of the cameras in harsh test environments—where the cameras may need to be operated remotely—each camera was configured with a fiber-optic link (including 30-m of optical cable) to the PC via the PixelVision custom PCI card. The fiber-optic coupling eliminates potential problems with *noisy* test environments; furthermore, the cameras and computer can be separated by large distances (e.g., 1 km). Each camera was equipped with a 35-mm-aperture Uniblitz mechanical shutter which has a minimum shuttering time of about 30 ms; also, the shutter can be triggered externally, to permit ease of synchronization with the firing of the Nd:YAG laser. Included with the cameras was the PixelView software for operating the cameras. The software was configured such that the cameras could be operated simultaneously, and images from both cameras were displayed within PixelView.

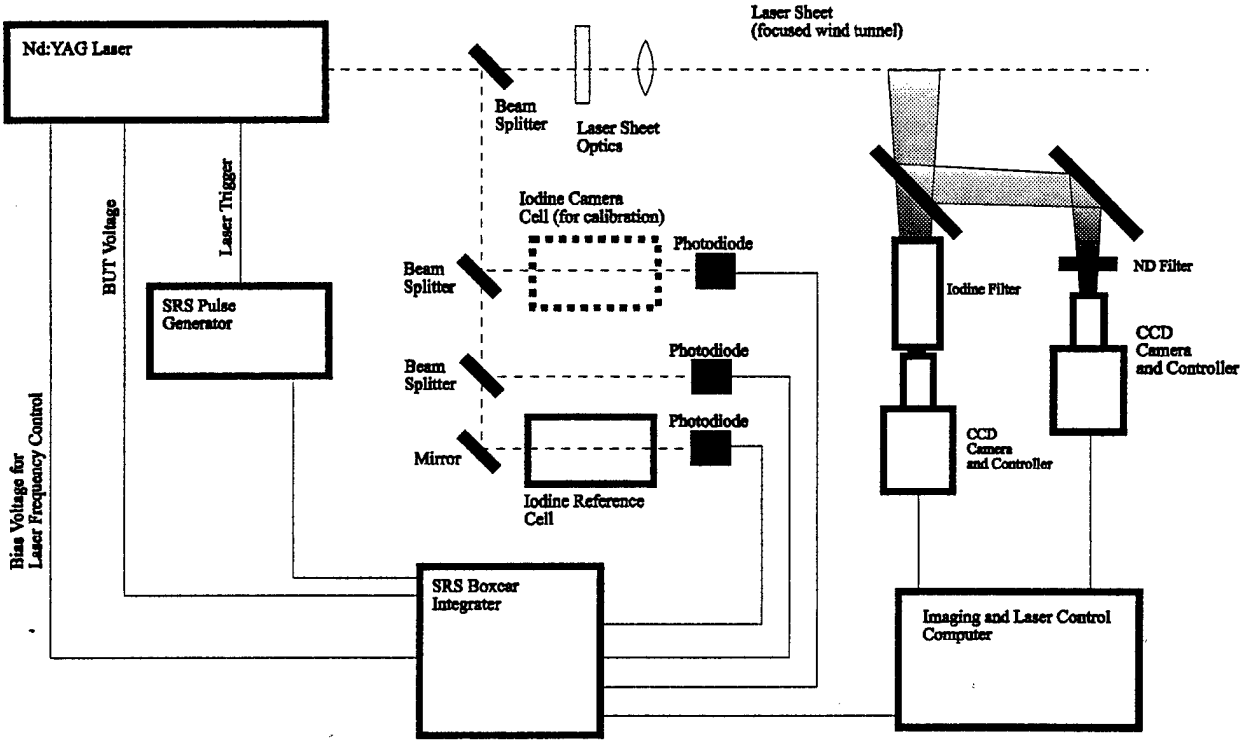

Figure 3. Schematic of laser and optical arrangement for FRS velocimetry measurements.

Custom Wavemeter

To effectively implement the FRS velocimetry technique, especially in low-speed flows where the Doppler shift is small, recording the laser wavelength on each laser shot is necessary. To implement a custom wavemeter, we used two Stanford Research Systems (SRS) gated integrators

(SR 250) along with an SRS computer interface (SR 245). With gated integrator, one selects sampling gates from 2 ns to 3 μs; the device then integrates the signal over this time period. As shown in Fig. 3, a small portion of the Nd:YAG beam (from an uncoated flat) was split off and directed to two fast photodiodes (1-ns rise time from Thor Labs); each photodiode was fitted with a flash opal diffuser for effective elimination of positional sensitivity of the photodiode output to the incoming light. One photodiode was employed to record the light transmitted by the reference I_2 filter, while the second photodiode acted as an absolute intensity reference. Of course, it is critical to ensure that the transition is not optically saturated (saturation occurs when the rate of pumping to the excited state becomes comparable to the rate of de-excitation, either through collisional quenching or fluorescence). Saturation results in a distorted I_2 transmission curve, and in the limit of complete saturation, the I_2-cell transmission approaches zero. Thus, to eliminate saturation, the laser beam was greatly expanded (to about 25 mm) using a Gallilean telescope. With this approach we then checked for saturation using calibrated neutral-density filters (the transmission should be independent of the laser energy entering the filter). A third gated integrator was employed in calibrating the reference I_2 filter relative to the camera I_2 filter.

Each photodiode signal was routed to a gated integrator where the photodiode current pulse was converted to a time-integrated high-impedance voltage. Typically, the sampling gates on the gated integrators were set to about 30 ns; triggering of these devices was provided by either a third photodiode (which provides the most stable trigger source) or an SRS DG535 digital delay generator. The gated-integrator voltages were digitized with a 13-bit resolution (12 bits plus a sign bit) using a SRS SR245 computer interface module. The SR245 is a flexible device that includes eight independently configurable ADC or DAC ports, two digital I/O ports, and an IEEE 488 interface (as well as an RS 232 interface) for communication with the PC.

Development of Software

For successful completion of the Phase I program, it was necessary to write custom software that would integrate the cameras with the custom wavemeter. Thus, using the Software Development Kit provided by PixelVision, we designed a Windows 95-based interface with the LabWindows/CVI (National Instruments) package. This interface routine included the following elements:

1) A routine for synchronizing operation of the cameras and the Stanford Research Systems gated integrators (custom wavemeter). The routine was designed to display the camera images side by side while also writing voltages recorded by the SR245 to the screen in either gray-scale or false-color formats. Subsequent to recording images, the user can easily zoom in on portions of the image. One of the eight ADC/DAC ports on the SR245 was dedicated to outputting a voltage to the seeder for controlling/setting the laser wavelength; of course, this voltage was user selectable (from −10 to +10 volts) within the interface routine. The format of the images was designed to be the same as that used by PixelView, to permit viewing the images with PixelView; a separate log file contains the simultaneously recorded voltages from the SR245.

2) Separate routines for operating the cameras or the wavemeter (gated integrators) alone. With the wavemeter interface, the outputs of the gated integrator were displayed graphically while the laser wavelength was scanned (with user-selectable voltage increments). Thus, I_2-filter transmission spectra were easily acquired; Figure 1 is an example of a *clean*, low-noise spectrum that was collected over the span of a few hours. The wavemeter-interface routine provided the option of averaging a given number of single-shot events, thus improving the precision of the measurements. Furthermore, the laser requires a characteristic "settling" time between wavelength increments; for the Nd:YAG laser employed in the SARL measurements, this amounted to about 5 sec for small wavelength increments.

3) A timing loop (with ~1-ms accuracy) for opening and closing the camera shutters synchronously with the arrival of the laser pulses within the probe volume. Both the shutter-open duration and the delay can be set independently. Once the controlling routine is ready to collect another image, it polls a digital I/O port on the SR245 for a laser-fire trigger pulse. Upon receipt of this signal, the program starts the timing sequence to open the camera shutters and acquire an image for the *next* laser pulse, arriving 100 ms after the triggering laser pulse. The TTL pulse controlling the operation of the shutters is derived from the second digital I/O port on the SR245.

In addition we also developed software to overlap images from the two cameras. An accurate overlapping of the arrays is a necessary first step to ratioing the images. The overlap process

involved analyzing images of a grid of alignment "dots" recorded with the two cameras. Once the FORTRAN routine is given a reference point, it then derives the set of coordinates matching the two images (of one CCD array relative to the other). As a test of the accuracy of the overlap routine, the "dot" array was translated by an arbitrary amount after recording an initial set of dot images. We then recorded a second set of dot images and compared the derived displacement for all pixels. The precision of this displacement was found to be within 0.15 pixels (i.e., this was the maximum deviation). Thus, we concluded that one can overlap the two images with ~0.1 pixel accuracy.

Demonstration and Testing

The demonstration and testing portion of the Phase I program included initial tests in an axisymmetric supersonic jet facility and subsequent testing/demonstration in the SARL facility. In all of our FRS velocity measurements, we tuned the Nd:YAG laser to the relatively isolated transition centered at 18789.28 cm^{-1} (Fig. 1); Gerstenkorn and Luc [1986] designate this transition of the B-X system of I_2 as the R121 line of the ($v'=35, v''=0$) band.

Axisymmetric Jet Facility

Initially, we tested the single-component FRS system employing a small-scale axisymmetric supersonic jet facility, with the purpose of evaluating different aspects of the system. Our tests included the following:

1) Investigation of the efficacy of a split-image format for *reference* and *filter* images. With the split-image approach, the *filter* and *reference* images are combined onto one CCD array, with the advantage of reduced cost (only one camera is required for each velocity component). However, unless the collected scattering has been collimated before splitting, the images combined on the CCD are overlapped to some degree. The overlap can be reduced by reducing the lens aperture; however, the reduced aperture tends to increase noise from speckle. Because of these limitations, we did not employ this split-image format and instead used separate *filter* and *reference* cameras.

2) Characterization of accuracy (for frame-averaged images) and precision (for individual images) of the derived velocity maps. In particular, we studied the effect of lens f/# on

speckle. With illumination of a "surface" having random phase aberrations (for example, a rough surface or, in our case, an ensemble of particles) by a spatially coherent source, a speckle pattern—resulting from constructive/destructive interference—is observed in the image plane [Reynolds et al., 1989]. Furthermore, this speckle noise recorded with the two cameras is largely uncorrelated (and, thus, adds in quadrature). We found speckle to be the primary source of noise for the instantaneous (i.e., single-shot) measurements of velocity for moderate-to-large Doppler shifts [McKenzie, 1996; Smith et al., 1996]. Because of the time-dependence of the seed density field, the speckle effect is absent (with a sufficient number of frames) in the frame-averaged measurements. In agreement with the studies of McKenzie [1996] and Smith et al. [1996], we found that as the lens aperture is increased, the radius of the diffraction blur spot decreases and consequently so does the speckle noise. Note also that in the Mach-1.36 jet, the frame-averaged velocities were within about 2% of the calculated value (for the jet core), while the RMS in the single-shot velocities within the jet core was about ~3.5%.

3) Analysis of the spectral purity of the Nd:YAG beam profile. That is, it has been reported that in injection-seeded Nd:YAG lasers, the frequency varies across the extent of the beam profile. Thus, we directed the beam to a diffuse surface and recorded images of the beam with the *filter* and *reference* cameras. Somewhat to our surprise, we found no measurable frequency variation across the beam profile for our laser system.

4) Testing and de-bugging of the camera/wavemeter software package. Improvements were then implemented based on this testing effort.

SARL Facility

This first-generation single-component instrument (including the injection-seeded laser system, cameras, I_2 filters, temperature controllers, wavemeter, PC, etc.) was moved to the SARL facility to demonstrate its efficacy in a realistic large-scale wind-tunnel facility. In particular, we recorded velocities above a delta wing with and without tail fins (Fig. 5). The leading-edge sweep on this model is 70°, and the tail shape is characteristic of an F-15 tail planform. Furthermore, the model has sharp leading edges on both the wing and tail surfaces for the purpose of fixing the separation points. The model was tested at a 23.2° angle of attack and with a free-

stream velocity of Mach 0.2; the corresponding root-chord-based Reynolds number was 1.94×10^6. At this condition and without the tails, no vortex bursting is observed; however, with the tails, the vortex bursts near the mid-chord location.

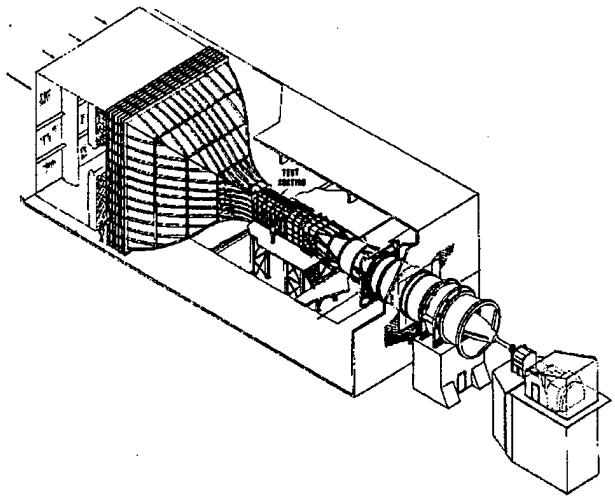

Figure 4. Subsonic Aerodynamic Research Laboratory (SARL) wind tunnel.

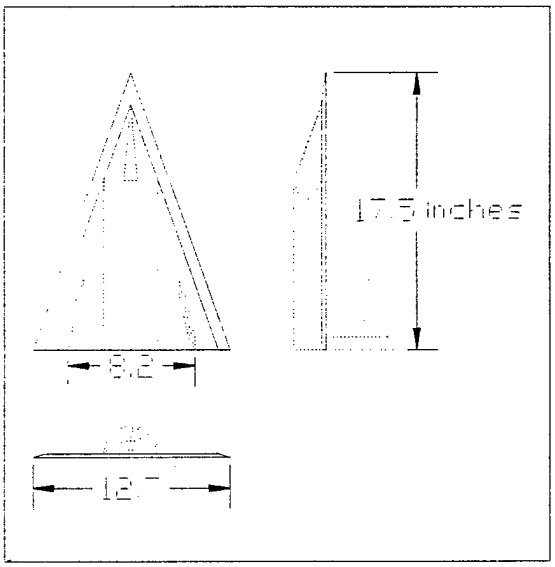

Figure 5. Delta-wing model with tails.

Figure 6 shows the layout of the major optical components (laser and camera) in relation to the wind tunnel and model for the velocity measurements described here. The Quanta-Ray GCR 150 injection-seeded laser, along with the custom wavemeter, were placed on a breadboard on top of the SARL facility; to dampen vibrations (which caused multi-mode lasing), we placed the

laser on foam packing material. This significantly improved the operation of the seeder; however,

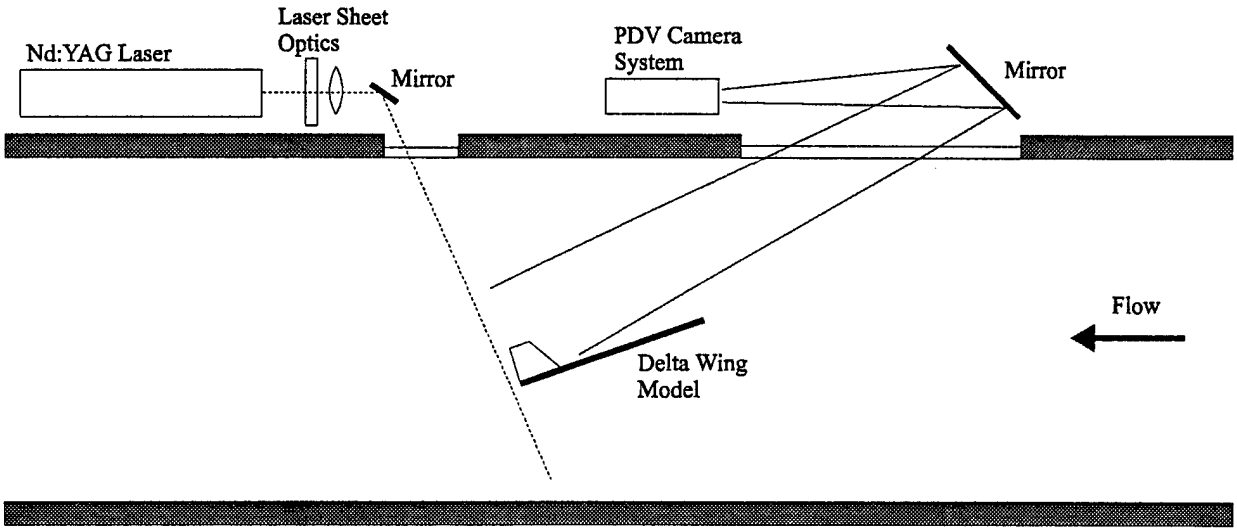

Figure 6. Experimental layout in the SARL wind tunnel.

an increased percentage of laser shots (compared to that observed in the laboratory) were not single mode. Thus, it was necessary to record the Q-switch build-up time, which is indicative of single-mode operation; this signal was also digitized with the SR245 interface.

The two PixelVision CCDs were also placed on top of the tunnel and viewed the laser scattering from a distance of about 4 m (Fig. 6); each camera was equipped with a Nikon Micro-Nikkor 105-mm f/2.8 lens and the resulting field of view of ~0.46 m. The FRS system was, thus, sensitive to the velocity component in the direction $-0.209\mathbf{i} - 0.003\mathbf{j} + 0.978\mathbf{k}$. Special care was taken to ensure that the two cameras viewed the imaged plane from the same angle, thus mitigating the angle sensitivity associated with Mie scattering. Also, we employed a polarization-insensitive beam-splitting cube to direct the scattering to both reference and filter cameras. A Stanford Research Systems DG535 pulse generator initiated the firing of the laser lamps and Q-switch and provided a synchronous trigger pulse to the SR245. Typically, the cameras were shuttered to about 60 ms, although somewhat shorter times are possible with the 35-mm-aperature Uniblitz shutters. Under test conditions where this shutter time is not sufficiently short to eliminate ambient light contamination, one can use Schott colored-glass filters or even an interference filter.

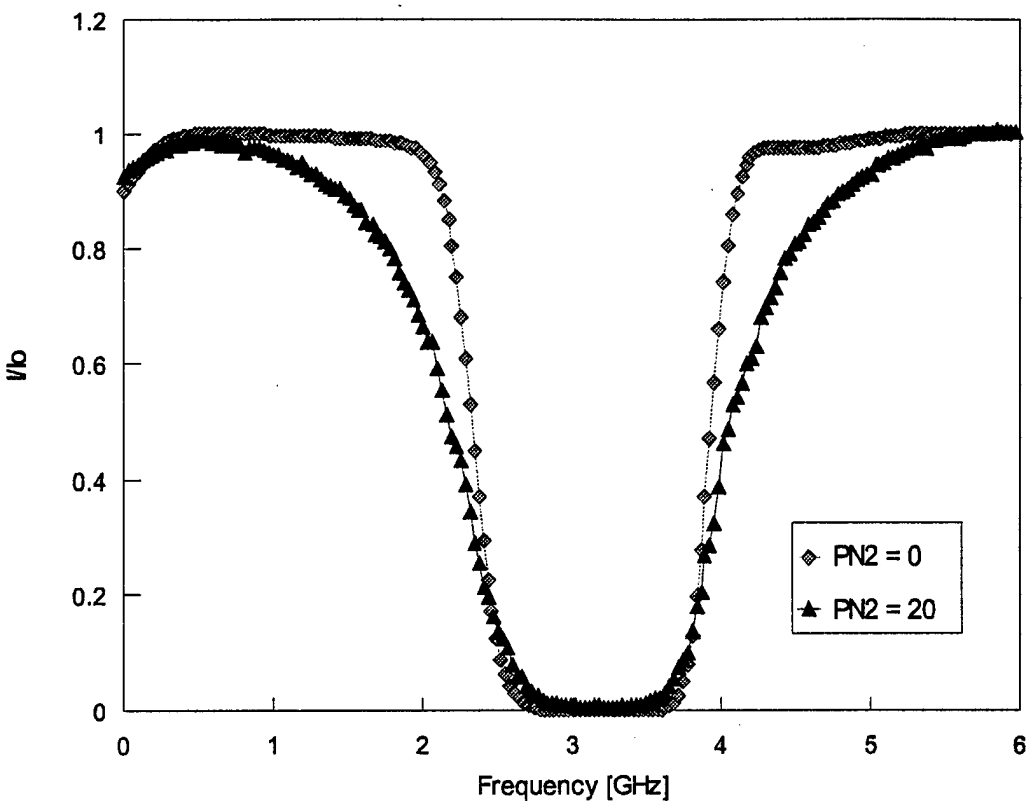

Figure 7. Pressure and Temperature broadened iodine transmission curves.

At the beginning of each day, we characterized the camera and wavemeter I_2 filters by scanning across the transition employed in this experiment and recording the transmission curve with the custom wavemeter. The difference in absorption profiles with and without pressure broadening with 20 Torr of nitrogen is clearly seen in Fig. 7. This filter-calibration procedure was a necessary step in relating the transmission recorded by the CCD to the frequency determined from the wavemeter. Note that the filters within the wavemeter and the one placed before the CCD were of different designs. The wavemeter filter, the first design type, included a water jacket with a reservoir of I_2 crystals; this I_2 reservoir is open to the main chamber of the cell, and the I_2 partial pressure within the chamber is controlled by the water-jacket temperature. Although the water-bath temperature is controlled within ±0.01 K (according to the manufacturer), presumably the jacket temperature is somewhat influenced by environmental conditions. The CCD filter, the second design type, has a valve between the I_2 crystal reservoir and the main chamber; once the I_2 partial pressure is set using the water bath and jacket, the valve to the I_2 reservoir is closed. Although setting the I_2 partial pressure is limited by the controllability of the

water-jacket temperature, the day-to-day repeatability of the cell conditions is much better. Although we had intended to employ two filters of this second type, only one was available at the time of the SARL test. Ultimately, the accuracy of the velocimetry measurements will be limited by the repeatability/stability of the cell conditions; of course, the cell design with the I_2-reservoir valve (the second type) is superior, insofar as repeatability is concerned.

We made initial measurements of the free-stream velocity (i.e., with the model removed) at Mach 0.2 and 0.3. The derived frame-averaged velocities were found to be within ~5% of the indicated (set) value determined from pitot probes; presumably, most of this error is due to the variation in I_2 side-arm temperature within the reference cell. The instantaneous velocity RMS for the SARL data is somewhat high, ~20%; our principal objective for the SARL tests, though, was on demonstrating the efficacy for the frame-averaged data. Nonetheless, assuming that the single-shot noise results from speckle, the precision of the single-shot velocities could be improved by employing a larger lens aperture (which was intentionally made small to improve the depth of field). However, the single-shot RMS may also be high as a result of laser unlocking effects that were more prevalent in the SARL.

Frame-averaged velocities are shown in Figs. 8 (without tails) and 9 (with tails). In both cases the image plane is normal to the wing and located 1.27 cm behind its downstream edge. Figure 8, which is the average of 62 single-laser-pulse images, shows two well-defined vortices indicated by a horizontal region with positive and negative peaks (associated with either side of the vortex). Figure 9, which is the average of 90 individual images, shows that the vortical structure is weaker for the delta wing with tails, because of vortex bursting. Note that in both cases, the velocity in the upper part of the field of view, away from the wing, approaches the value expected for the freestream velocity component, ~37 m/s. Velocity images were recorded at three additional locations. Note also that timely analysis (completed the evening of the tunnel run) of the Phase I SARL data allowed us to diagnose potential problems more quickly, thereby improving the accuracy of the velocities.

A paper describing the flowfield, based on the complete data set and a comparison with the numerical solution, will be presented at the 20th AIAA Advanced Measurement and Ground Test Technology Conference in Albuquerque, NM (June 15-18, 1998) [Beutner et al., 1998]. A

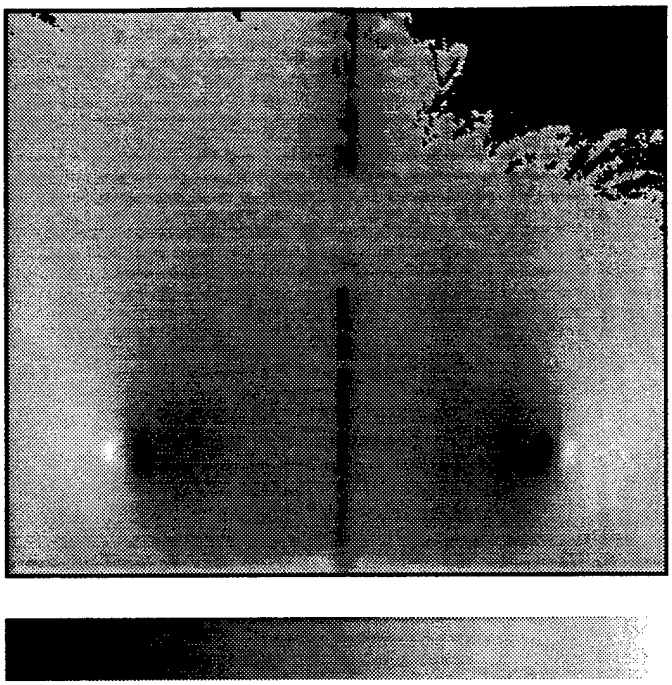

-120 40 m/s

Figure 8. Average velocity component above a delta-wing without tail fins.

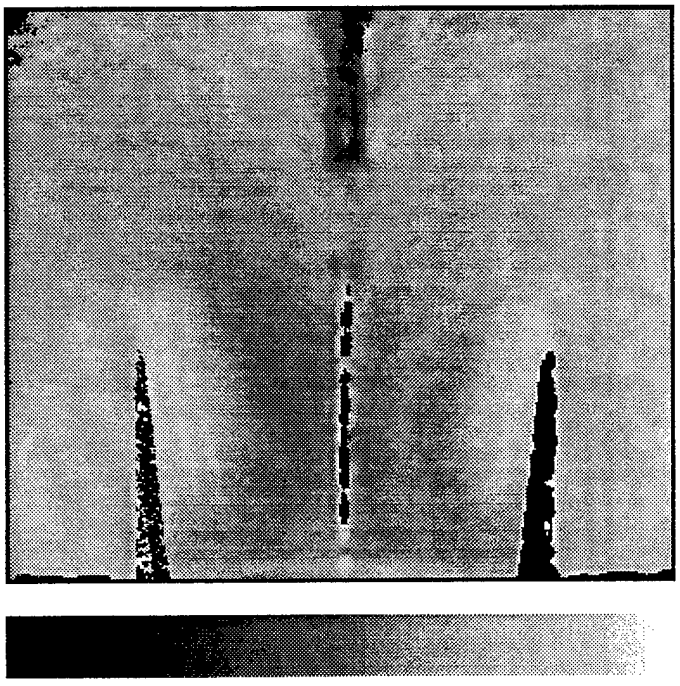

-120 40 m/s

Figure 9. Frame-averaged velocity component above a delta-wing with tail fins.

second paper focusing on the FRS technique (describing limitations, accuracy, etc.) will be presented at the 29th AIAA Fluid Dynamics Conference [Mosedale et al., 1998].

3. POTENTIAL APPLICATIONS

Many advanced aerodynamic design concepts—boundary-layer control through the use of MEMs (micro electro-mechanical) devices, leading-edge blowing, synthetic jets, juncture and corner flows, etc.—result in complex, unsteady flowfields which are currently difficult or impossible to model. Even in cases where computational modeling is feasible, validation is a critical step in the design process. In both cases, reliable and efficient evaluation of new aerodynamic designs will depend on the development of likewise reliable and efficient—and, therefore, cost-effective—wind-tunnel instrumentation (i.e., instrumentation that can be implemented on a larger scale than competing instruments based on PIV and PLIF). First, the advanced diagnostic developed under this SBIR program will have a significant impact on the advancement of aerodynamic systems, benefiting the research and development programs in both commercial- and military-aircraft industries. Second, R&D laboratories (both Academic and Industrial) concerned with the characterization of moderate- or high-speed unsteady flows (e.g., the automotive industry) can benefit from this technology. Finally, other ongoing and/or recently initiated programs such as DOD's IHPTET and HyTech programs and NASA's High Speed Civil Transport can also profit from the development program for FRS velocimetry.

4. REFERENCES

Beutner, T. J., Elliott, G., Mosedale, A., Carter, C., "Doppler Global Velocimetry Applications in Large Scale Facilities," To be presented at the 20th AIAA Advanced Measurement and Ground Testing Conference, Albuquerque, NM (June 15-18, 1998).

Gerstenkorn, S. and Luc, P., Atlas du Spectre d' Absorption de la Molecule d' Iode: 14800-2000 cm^{-1}, Publication of C.N.R.S. Laboratorie AIME-COTTON, C.N.R.S., II –91405, Orsay, France, 1986.

McKenzie, R. L., "Measurement Capabilities of Planar Doppler Velocimetry Using Pulsed Lasers," *Applied Optics*, Vol. 35, No. 6, pp. 948-964, 1996.

Meyers, J. F., and Komine, H., "Doppler Global Velocimetry: A New Way to Look at Velocity," *Laser Anemometry*, Vol. 1, pp. 289-296, 1991.

Miles, R. B., Lempert, W. R., and Forkey, J., "Instantaneous Velocity Fields and Background Suppression by Filtered Rayleigh Scattering," AIAA Paper 91-0357, January 1991.

Miles, R. B., Forkey, J. N., and Lempert, W. R., "Filtered Rayleigh Scattering Measurements in Supersonic/Hypersonic Facilities," AIAA Paper 92-3894, January 1992.

Mosedale, A., Elliott, G., Carter, C., and Beutner, T., "On the use of Planar Doppler Velocimetry," To be presented at the 29th AIAA Fluid Dynamics Conference, Albuquerque, NM (June 15-18, 1998).

Reynolds, G. O., DeVelis, J. B., Parrent, G. B., Thompson, B. J., *The New Physical Optics Notebook: Tutorials in Fourier Optics*, SPIE—The International Society for Optical Engineering, Bellingham, WA, 1989.

Shimizu, H., Lee, S. A., and She, C. Y., "High Spectral Resolution LIDAR System with Atomic Blocking Filters for Measuring Atmospheric Parameters," *Applied Optics*, Vol. 22, pp. 1373-1381, 1983.

Smith, M. W., and Northam, G. B., and Drummond, J. P. "Application of Absorption Filter-Planar Doppler Velocimetry to Sonic and Supersonic Jets," *AIAA Journal*, Vol. 34, No. 3, pp. 434-441, 1996.